



PCCP

Anionic Derivatives of Uracil: Fragmentation and Reactivity

Journal:	<i>Physical Chemistry Chemical Physics</i>
Manuscript ID:	CP-ART-05-2014-002277
Article Type:	Paper
Date Submitted by the Author:	23-May-2014
Complete List of Authors:	Cole, Callie; University of Colorado at Boulder, Department of Chemistry and Biochemistry Wang, Zhe-Chen; University of Colorado at Boulder, Department of Chemistry and Biochemistry Snow, Theodore; University of Colorado at Boulder, Astrophysical and Planetary Sciences; University of Colorado at Boulder, Center for Astrophysics and Space Astronomy Bierbaum, Veronica; University of Colorado at Boulder, Department of Chemistry and Biochemistry; University of Colorado at Boulder, Center for Astrophysics and Space Astronomy

SCHOLARONE™
Manuscripts

Anionic Derivatives of Uracil: Fragmentation and Reactivity

Cite this: DOI: 10.1039/x0xx00000x

Callie A. Cole,^a Zhe-Chen Wang,^a Theodore P. Snow^{bc} and Veronica M. Bierbaum^{ac}

Received 00th XXXXXX 2014,
Accepted 00th XXXXXX 2014

DOI: 10.1039/x0xx00000x

www.rsc.org/

Uracil is an essential biomolecule for terrestrial life, yet its prebiotic formation mechanisms have proven elusive for decades. Meteorites have been shown to contain uracil and the interstellar abundance of aromatic species and nitrogen-containing molecules is well established, providing support for uracil's presence in the interstellar medium (ISM). The ion chemistry of uracil may provide clues to its prebiotic synthesis and role in the origin of life. The fragmentation of biomolecules provides valuable insights into their formation. Previous research focused primarily on the fragmentation and reactivity of cations derived from uracil. In this study, we explore deprotonated uracil-5-carboxylic acid and its anionic fragments to elucidate novel reagents of uracil formation and to characterize the reactivity of uracil's anionic derivatives. The structures of these fragments are identified through theoretical calculations, further fragmentation, experimental acidity bracketing, and reactivity with several detected and potential interstellar species (SO₂, OCS, CS₂, NO, N₂O, CO, NH₃, O₂, and C₂H₄). Fragmentation is achieved through collision induced dissociation (CID) in a commercial ion trap mass spectrometer, and all reaction rate constants are measured using a modification of this instrument. Experimental data are supported by theoretical calculations at the B3LYP/6-311++G(d,p) level of theory. Lastly, the astrochemical implications of the observed fragmentation and reaction processes are discussed.

1. Introduction

Research in astrobiology and the origin of life is contingent upon an understanding of the chemistry of nucleobases. Uracil is a pyrimidine nucleobase that makes up ribonucleic acid (RNA), theorized to be the predecessor of deoxyribonucleic acid (DNA) and key to the RNA World hypothesis.¹ According to one theory for the origin of life, prebiotic organics were delivered to the early earth by comets or meteorites.²⁻⁴ This theory suggests that the first biomolecules were exogenously synthesized, motivating extensive research on the prebiotic formation of biomolecules such as uracil in three interstellar nurseries for complex organic molecules: the gas-phase, grain surfaces, and ice mantles.⁵ Many different formation routes to uracil such as the incorporation of HCN into aromatic species,⁶ the reactions of cyano molecules,⁷⁻⁹ and the ultraviolet photochemistry induced in water mixtures^{10, 11} have been proposed. The tentatively-detected interstellar molecule urea¹² has also been suggested as a uracil precursor.^{13, 14} Recent astrochemical interest in small N-containing neutral molecules and ions has increased due to their potential to form more complex biomolecules.^{15, 16} Although the studies in this field on neutral and cationic species are exhaustive, the anionic chemistry of uracil remains largely missing from proposed syntheses. Our previous research has shown, however, that the

chemistry of negative ions can be remarkably important in the interstellar medium (ISM).^{17, 18}

Uracil is the only pyrimidine nucleobase that has been detected in all three of the Murchison, Murray, and Orgueil carbonaceous meteorites,^{10, 19-21} providing an important piece of evidence for the theory of exogenous synthesis and delivery to early earth. Motivated by these detections, the abundance of interstellar nitrogen, and the known predominance of interstellar aromatic molecules,²² astronomical searches for nucleobases have been extensive.²³⁻²⁸ In spite of these efforts, no N-heterocycles including nucleobases have been conclusively detected in the ISM to date.²² Currently, an upper limit has been placed on the column density of pyrimidine, and the astronomical search continues.²⁹

Biomolecule dissociation is vital to the prediction of prebiotic formation routes.^{30, 31} The reactivity of biomolecule fragments is also essential to this end. In this study, we expand our previous work on the interstellar formation pathways,^{32, 33} reactivity,³⁴ and fragmentation³⁵ of complex interstellar organics through an analysis of uracil and its anionic derivatives. Former fragmentation studies on uracil involve primarily cations, ranging from protonated species^{36, 37} to metal cation complexes.³⁸ Ionization and fragmentation have been accomplished by energetic interactions of photons,³⁹ electrons,⁴⁰

protons,⁴¹ and ions⁴² with uracil molecules. Anionic species derived from uracil fragmentation remain largely unexplored. In a recently-modified Finnigan LCQ Deca XP Plus ion trap apparatus, we examine several anions produced by the ionization and subsequent fragmentation of uracil-5-carboxylic acid.

The structures of the ions are determined by consecutive collision induced dissociation (CID), acidity bracketing, and theoretical calculations. In this study we produce OCN^- , a known substituent of interstellar ices,⁴³ directly from deprotonated uracil. Imidoylketene, a molecule of cosmological interest that has been largely overlooked for decades,⁴⁴ is the other key fragment of deprotonated uracil. Imidoylketene has been computationally shown to react to form cyclic, aromatic structures similar to uracil,⁴⁵ yet no reports to date have suggested this molecule as a precursor to uracil itself. The positive interstellar detection of its isomer, oxiranecarbonitrile, provides encouraging evidence for the future discovery of imidoylketene.^{46, 47} The two fragments that are derived from deprotonated uracil, therefore, are both likely interstellar species and may be involved in larger biomolecule formation in ice mantles, or other environments where complex organics are predicted to survive. In addition to fragmentation, we report the rate constants and reaction efficiencies of deprotonated imidoylketene with several detected and potential interstellar species (SO_2 , OCS , CS_2 , NO , N_2O , CO , NH_3 , O_2 , and C_2H_4). Our overall goal is to illustrate the role of anion dissociation and reactivity in the formation of more complex biomolecules of astrobiological relevance.

2. Experimental Methods

Experimental data are gathered using a modified Finnigan LCQ Deca XP Plus ion trap. This instrument has been described in our previous work,³⁵ and is outlined here in brief. Ions are generated from an electrospray ionization (ESI) source with a spray voltage of 4.5 kV, a flow of 5–10 $\mu\text{L min}^{-1}$, and heated capillary temperatures of 200–250 °C. The electrospray solution consists of 10^{-4} M uracil-5-carboxylic acid (97+%, Alfa Aesar) in a solvent mixture of 1:1 $\text{CH}_3\text{OH}:\text{H}_2\text{O}$ (HPLC grade, Sigma-Aldrich). The ions formed from the ESI source are injected into the ion trap where they are collisionally thermalized by helium at 5.1×10^{-3} Torr.⁴⁸ Multiple CID events (MS^n) are then possible by applying appropriate resonance excitation RF voltages to the endcap electrodes of the trap. For all dissociations performed in this study, we apply a normalized collision energy (NCE) of 40–70% for a duration of 20–50 ms to optimize fragment ion signal. Figure 1 outlines the formation of deprotonated uracil-5-carboxylic acid from the solution containing uracil-5-carboxylic acid by ESI. Our previous work³⁵ and that of others^{49, 50} often involve molecules whose most acidic site is on the carboxylic acid group itself. Here, the N_1 site is the most acidic, yielding parent anions that are predominantly deprotonated there. CID on this ion involves several processes including decarboxylation, which are examined in depth in the following sections.

The parent or fragment ions may be isolated within the ion trap between 1 and 5000 ms. Over this time range, we are able to monitor reactions between these ions and neutral reagents that are introduced through the pre-existing helium buffer gas line. The modifications required to introduce these reagents are based on those of Gronert and

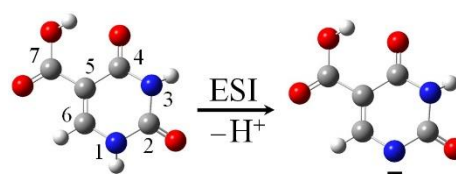


Figure 1. Uracil-5-carboxylic acid is deprotonated upon ESI at the most acidic site, N_1 .

coworkers.⁵¹ Helium (UHP, 99.999%, Airgas) is maintained at a constant flow between 1.0–1.9 L min^{-1} using a flow controller through a line external to the ion trap. Within this line, the pressure is maintained at 850 Torr ($\pm 3\%$). Only a small fraction (0.1%)⁵² of this helium-reagent mixture is sampled through fused silica capillary tubing into the ion trap itself. Gaseous neutral reagents are purchased as dilute mixtures ($1.00 \pm 0.02\%$) in helium (OCS , SO_2 , Airgas) and added into the helium line. Other gases that showed no reactivity were not purchased diluted in helium (N_2O , O_2 , C_2H_4 , and CO , 99.5%; NO and HCl , 5% in helium; and NH_3 , 99.9995%, Airgas). Volatile liquid neutral reagents are introduced into the helium line by syringe pump (0.5–5.0 $\mu\text{L min}^{-1}$). The liquid reagents used in this study include carbon disulfide >99%, pyrrole 98%, 2,2,3,3,3-pentafluoro-1-propanol 97%, liquefied phenol >85%, propionic acid >99.5%, thiophenol >99%, aniline $\geq 99.5\%$, and aqueous HBr 48% purchased from Sigma-Aldrich, acetone 99.7% from Fisher Scientific, and acetone- d_6 99.5% from Cambridge Isotope Laboratories, Inc.

Reaction kinetics data are determined using pseudo-first order kinetic analyses and by measuring the decline in reagent ion signal at six or more separate reaction times (1–5000 ms). Ion trap rate constants are calibrated against flowing afterglow-selected ion flow tube (FA-SIFT) measurements^{53, 54} and agree within the expected experimental uncertainties for gas-phase ion kinetics ($\pm 20\text{--}30\%$).⁵¹ Lastly, all experimental data reported here are the averages of six data points taken over two days with a minimum of three different helium:reagent ratios to ensure reproducibility over a range of experimental conditions.

3. Theoretical Calculations

Experiments in this study are complemented by ab initio calculations performed using the *Gaussian 03* and *Gaussian 09* suites of programs.^{55, 56} Enthalpies are reported at 0 K for all reaction and fragmentation pathways. All transition states (TS) reported within these pathways are verified by forward and reverse intrinsic reaction coordinate analyses. Gas-phase acidities are calculated and reported as the change in the enthalpy for reaction (1) at 298 K, where AH represents the molecule of interest.



The B3LYP/6-311++G(d,p) level of theory is used for all geometry optimizations and frequency calculations. Associated zero point energy (ZPE) and thermal energy (298 K) corrections are applied as specified.

4. Results and Discussion

4.1 Fragmentation

Decarboxylation is not the exclusive CID pathway for deprotonated heterocyclic carboxylic acids. For example, our recent study on deprotonated isoxazole revealed that HCN loss and CO₂ loss occur together.³⁵ Analogous to this process, deprotonated uracil-5-carboxylic acid involves two competing fragmentation channels: decarboxylation and isocyanic acid (HNCO) loss, which result in three fragment ions (structures II-IV, Figure 2).

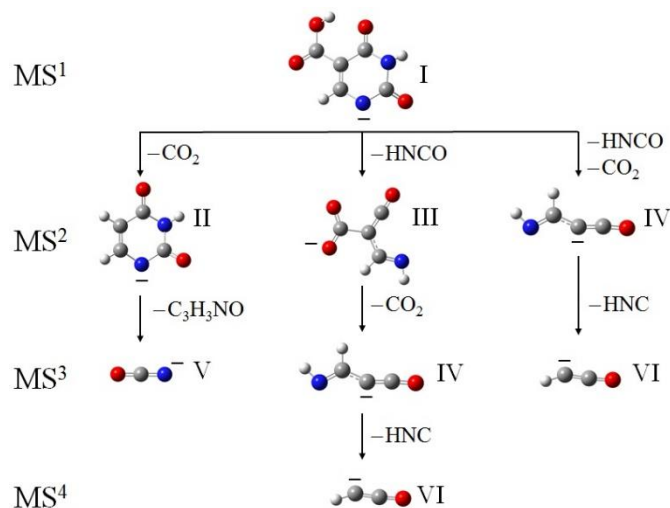


Figure 2. Proposed structures that arise from the fragmentation of deprotonated uracil-5-carboxylic acid (I) are summarized by collision event (MS¹–MS⁴). Deprotonated uracil (II), deprotonated imidoylketene carboxylic acid (III), deprotonated imidoylketene (IV), OCN[−] (V) and HC₂O[−] (VI) are all derived from these fragmentation processes.

The overall breakdown of deprotonated uracil-5-carboxylic acid (I, C₅H₃N₂O₄[−]) is summarized in the series of collision events shown in Figure 2 (MS¹–MS⁴). The initial CID process involves decarboxylation to form deprotonated uracil (II, C₄H₃N₂O₂[−]), isocyanic acid (HNCO) loss to form deprotonated imidoylketene carboxylic acid (III, C₄H₂N₂O₃[−]), and losses of both CO₂ and HNCO yielding deprotonated imidoylketene (IV, C₃H₂N₂O[−]). The following sections detail our structural identification of each of these fragments. The third (MS³) and fourth (MS⁴) CID processes provide evidence for specific parent ion structures. Briefly, C₄H₃N₂O₂[−] (II) yields OCN[−], suggesting an N-deprotonated rather than a C-deprotonated parent ion. C₄H₂N₂O₃[−] (III) produces IV, indicating a decarboxylation process and likely a carboxylic acid parent ion. Finally, C₃H₂N₂O[−] (IV) fragments to form HC₂O[−] in both cases, strongly indicating that the C₃H₂N₂O[−] (IV) species from both CID sequences are identical. Further computational and experimental analyses are given in the following sections to verify the fragment structures shown here.

4.2 Structural Identification

Parent and fragment ions in this study may tautomerize and isomerize under CID conditions, increasing the number of possibilities of fragmentation pathways and structures. This section outlines the expected structures for each experimentally-observed mass-to-charge ratio. An approach comprised of theoretical calculations, experimental acidity bracketing, and consecutive fragmentation is used to tease apart the most viable structure of each fragment.

4.2.1 Deprotonated uracil-5-carboxylic acid (I) The mechanism of ESI has been shown to deprotonate large biomolecules at multiple sites,⁵⁷ although the most acidic site is energetically favoured.⁵⁸ At the B3LYP/6-311++G(d,p) level of theory, we have calculated the ZPE corrected electronic energies of 19 isomers of deprotonated uracil-5-carboxylic acid (Figure S1), ten of which are shown in Figure 3a. Additionally, we have calculated the acidity of each viable deprotonation site. The most stable anion is the N₁ deprotonated structure (II; ΔH^o_{acid}=315.5 kcal mol^{−1}). Approximately 9 kcal mol^{−1} higher in energy is the N₃ deprotonated species (ΔH^o_{acid}=325.0 kcal mol^{−1}). Interestingly, deprotonating uracil-5-carboxylic acid at the carboxylic acid group itself produces a structure 22 kcal mol^{−1} less stable and is much less acidic than that of the N₁ site (ΔH^o_{acid}=337.4 kcal mol^{−1}). This is in part due to intramolecular hydrogen bonding between the carboxylic acid hydrogen and the oxygen of the adjacent carbonyl group of the parent molecule (Figure 1). Many tautomers and isomers, as Figure 3a illustrates, are accessible within 50 kcal mol^{−1} of the most stable species (I). For this reason, we have experimentally bracketed the acidity of this ion to validate our assertion that ESI of a solution of uracil-5-carboxylic acid preferentially produces the N₁ deprotonated anion.

Using the known experimental acidities of several reagents,⁵⁹ we observed the reactivity of C₅H₃N₂O₄[−] with an array of neutral molecules in our modified ion trap apparatus. The acidity bracketing data are summarized in Table 1 for C₅H₃N₂O₄[−], C₄H₃N₂O₂[−], and C₃H₂N₂O[−] (the latter two are outlined in the following sections). This experiment involves trapping each ion (R[−]) in the presence of the neutral molecules (AH) listed in Table 1. This table indicates the positive or negative detection of the A[−] proton abstraction product (with a Y or N, respectively). Had the structure of C₅H₃N₂O₄[−] contained a mixture of isomers such as those listed in Figure 3a, we would expect to observe reactivity with one or more of these neutral reagents. Rather, we do not observe the formation of any product ions (A[−]). Our calculated acidity of the N₁ site of uracil-5-carboxylic acid is 315.5 kcal mol^{−1}, whereas alternative deprotonation sites on uracil-

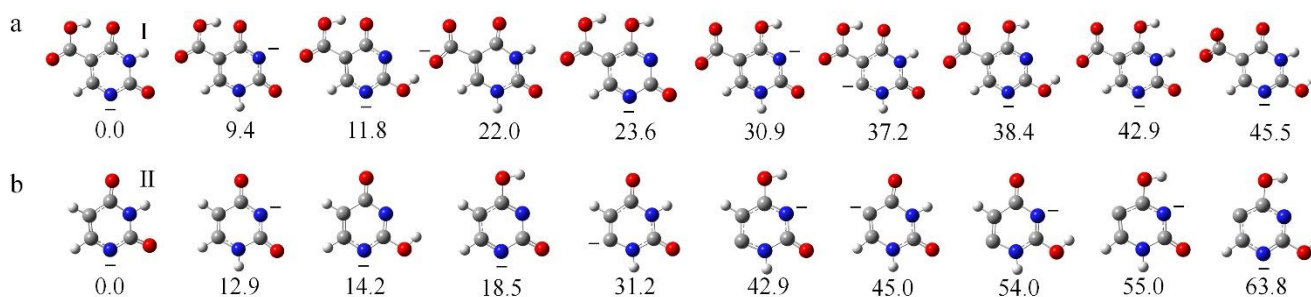


Figure 3. Several possible isomeric structures of $C_5H_3N_2O_4^-$ (a) and $C_4H_3N_2O_2^-$ (b) are listed in order of increasing electronic energies (ZPE corrected) relative to the most stable isomer. These energies (kcal mol^{-1}) are calculated at the B3LYP/6-311++G(d,p) level of theory and shown beneath each structure. N_1 deprotonated uracil-5-carboxylic acid (I) and N_1 deprotonated uracil (II) are the most stable structures. (Additional structures of each ion have been optimized and are included in Figures S1 and S3).

5-carboxylic acid are much less acidic ($\geq 325.0 \text{ kcal mol}^{-1}$). Our results (Table 1) indicate that $C_5H_3N_2O_4^-$ is in fact more acidic than hydrobromic acid, generating an experimental upper limit of $\Delta H^\circ_{\text{acid}} < 323.540 \pm 0.050 \text{ kcal mol}^{-1}$, in agreement with our theoretical value for the N_1 deprotonated species (I).

The CID pathways accessible to uracil molecules are often defined by their ease of tautomerization and isomerization.³⁷ Many of the structures listed in Figure 3a are accessible by pathways with barriers readily overcome under CID conditions ($\leq 50 \text{ kcal mol}^{-1}$; Figure S2). Figure 4 includes a potential CID process to form fragments II-IV from I. Decarboxylation occurs directly from structure I, yielding II by way of a $50.9 \text{ kcal mol}^{-1}$ transition state. In contrast to this direct process, we propose that I isomerizes into a species deprotonated at the carboxylic acid site ($+22.0 \text{ kcal mol}^{-1}$, Figure 3a) prior to fragmenting into III and IV. This isomerization process is represented by a dashed line in the figure, and is included in supporting information (Figure S2). Considering the barriers of isomerization are lower than the barriers to isocyanic acid (HNC) loss ($63.5 \text{ kcal mol}^{-1}$), these rearrangements likely occur prior to this process.

4.2.2 N_1 deprotonated uracil (II) As Figure 4 demonstrates, deprotonated uracil ($C_4H_3N_2O_2^-$) is produced by decarboxylation of deprotonated uracil-5-carboxylic acid ($C_5H_3N_2O_4^-$) upon CID.

Similar to its parent, however, deprotonated uracil has many tautomers and isomers which may be accessible through CID. Ten of these structures are shown in Figure 3b (a more extensive list is included in Figure S3). Due to the direct CID pathway from the parent ion (I) to N_1 deprotonated uracil (II) as well as its overall stability, this structure is reasonably in highest abundance. Next higher in energy is its N_3 deprotonated counterpart ($+12.9 \text{ kcal mol}^{-1}$), followed by two N_1 deprotonated tautomers ($+14.2$ and $+18.5 \text{ kcal mol}^{-1}$, respectively). Even less stable are the C_6 ($+31.2 \text{ kcal mol}^{-1}$) and C_5 ($+45.0 \text{ kcal mol}^{-1}$) deprotonated ions and their associated tautomers. To clearly delineate which structure is produced from CID, we have performed another series of bracketing experiments, included in Table 1 under $C_4H_3N_2O_2^-$.

Our experimental results suggest that the most stable ion, N_1 deprotonated uracil (II), is formed in our apparatus. The acidities ($\Delta H^\circ_{\text{acid}}$) of different sites on uracil have previously been calculated by the Kenttämäa research group to be 332.8 ± 2.2 , 345.1 ± 2.2 , 380.2 ± 0.5 , and $366.2 \pm 0.5 \text{ kcal mol}^{-1}$ for the N_1 , N_3 , C_5 , and C_6 sites, respectively.⁶⁰ Using these data and the known experimental acidities of the aforementioned reagents,⁵⁹ we observed the reactivity of $C_4H_3N_2O_2^-$ (Table 1). Hydrochloric and hydrobromic acids reacted with this ion to produce Cl^- and Br^- products, but no products were observed for the less acidic reagents. Therefore, the acidity of the

Table 1. Qualitative Bracketing Results¹

AH	$\Delta G^\circ_{\text{acid}}(\text{AH})^2$	$\Delta H^\circ_{\text{acid}}(\text{AH})^2$	R ⁻		
			$C_5H_3N_2O_4^-$	$C_4H_3N_2O_2^-$	$C_3H_2NO^-$
Acetone ³	361.9 ± 2.0	368.8 ± 2.1	N	N	N
Aniline	359.1 ± 2.0	366.4 ± 2.1	N	N	N
Pyrrole	350.9 ± 2.0	359.54 ± 0.25	N	N	N
2,2,3,3,3-Pentafluoro-1-propanol	348.8 ± 6.0	355.4 ± 6.1	N	N	Y
Phenol	342.3 ± 2.0	349 ± 2	N	N	Y
Propionic Acid	340.4 ± 2.0	347.4 ± 2.2	N	N	Y
Thiophenol	333.4 ± 2.1	340.4 ± 2.1	N	N	Y
Hydrochloric Acid	328.10 ± 0.10	333.40^4	N	Y	Y
Hydrobromic Acid	318.30 ± 0.15	323.540 ± 0.050	N	Y	Y

¹ $R^- + AH \rightarrow RH + A^-$

²All values are given in kcal mol^{-1} and obtained from the NIST WebBook.⁵⁹

³Acetone-d₆ was also studied and no reactions were observed.

⁴Error bars are not specified in the NIST WebBook.

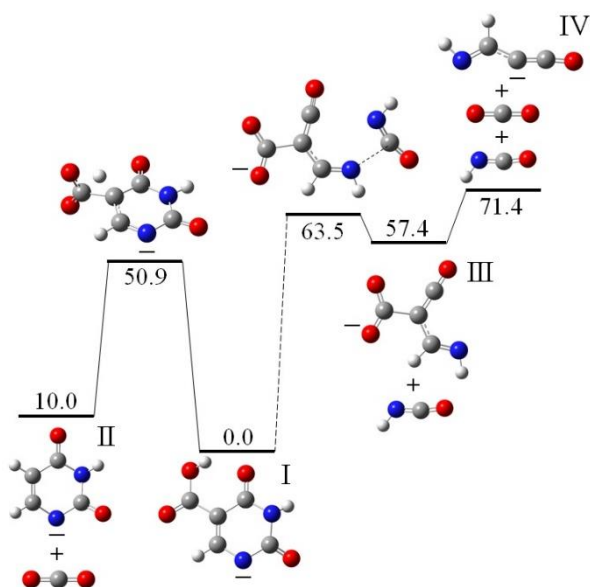


Figure 4. Possible pathways (kcal mol⁻¹) calculated at the B3LYP/6-311++G(d,p) level of theory are shown for the CID of N₁ deprotonated uracil-5-carboxylic acid (I) to produce anions II-IV. The dashed line indicates the isomerization of I prior to further fragmentation. A potential energy surface of the isomerization process of I is included in Figure S2.

anion is 336.9 ± 2.1 kcal mol⁻¹ according to our bracket, in agreement with the N₁ results of the Kenttämaa group.

A further verification of these results is required, due to a process previously observed in our research⁶¹ involving the isomerization of anions upon reaction with an acid. Briefly, the anions that we are bracketing may originate as a more basic structure (shown in Figures 3a and 3b). For example, C₅ deprotonated uracil would readily abstract a proton from an acid AH to form an ion-neutral complex of uracil and A⁻ as shown in equation (2); however, before separation of the complex, A⁻ can abstract a proton from the most acidic site of uracil to form N₁ deprotonated uracil (II). This isomerization produces no change in the mass of the ion, making the ion appear unreactive with AH.



If the parent ion is deprotonated at the carboxylic acid site (+22.0 kcal mol⁻¹, Figure 3a), it would readily decarboxylate under CID to form C₅ deprotonated uracil (+45.0 kcal mol⁻¹, Figure 3b). To test whether an acid-catalyzed isomerization is taking place, we use acetone-d₆ as an additional bracketing reagent (Table 1). If C₅ deprotonated uracil is present in our apparatus, the acetone would deuterate the C₅ site before abstracting a proton from the N₁ site, producing an ion with 1 amu higher mass. We did not observe a deuterated product from the reaction of acetone-d₆ with C₄H₃N₂O₂⁻. This provides additional support that our structural identifications of I and II are correct, and no acid-catalyzed isomerization is taking place.

Lastly, II forms a single ionic product when fragmented: OCN⁻. We have inferred the neutral product, imidoylketene, and the potential energy diagram of this dissociation process is provided in Figure 5.

Analogous to the fragmentation of I in Figure 4, the lowest energy CID pathway for II involves isomerization. The initial conversion of N₁ to N₃ deprotonated uracil prior to fragmentation allows a low energy (33.7 kcal mol⁻¹) dissociation of the N₁-C₂ bond leading to OCN⁻ and imidoylketene, a total of 53.4 kcal mol⁻¹ higher in energy than II. We expand on the astrochemical relevance of these products in an upcoming section.

4.2.3 Deprotonated imidoylketene (IV) The remaining two fragments of deprotonated uracil-5-carboxylic acid, III and IV, are formed by means of isocyanic acid (HNCO) loss. As shown in Figure 4, structure III leads to IV and will therefore be implicit in our discussion of the formation and structure of IV. We began with an overall examination of several ring-closed and ring-opened candidates for C₃H₂NO⁻. Although ring structures have been proposed in previous investigations of protonated uracil fragments,³⁷ we do not expect that the analogous deprotonated ring species will be formed here due to their instability (≥ 47.3 kcal mol⁻¹) relative to IV. Although more stable isomers of IV do exist, they cannot be formed directly from I without significant rearrangements.

Experimental bracketing results similarly indicate that IV is a reasonable structure. As Table 1 demonstrates, our experimental bracket of C₃H₂NO⁻ gives an acidity ($\Delta H^{\circ}_{\text{acid}}$) of 357.5 ± 6.1 kcal mol⁻¹. The calculated acidity of IV at the B3LYP/6-311++G(d,p) level of theory is 349.5 kcal mol⁻¹. Although this result is slightly lower than our experimental bracket, these values are in reasonable agreement due to the known underestimation of thermochemical values by density functional theory.⁶²

The fragmentation processes leading to and from C₃H₂NO⁻ provide deeper insights into the feasibility of structure IV. Only one daughter ion, HC₂O⁻, is formed from the CID of C₃H₂NO⁻ (Figure 2). The formation of this ion from IV involves one H transfer: minimal

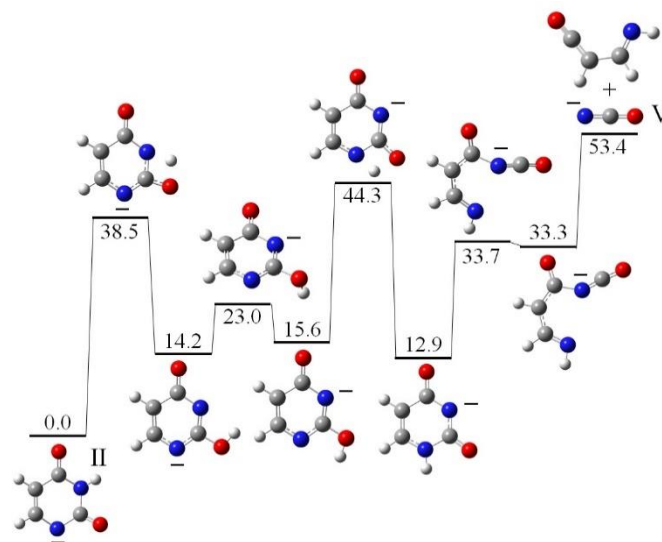


Figure 5. A pathway (kcal mol⁻¹) calculated at the B3LYP/6-311++G(d,p) level of theory is shown for the CID of N₁ deprotonated uracil (II). OCN⁻ and the inferred neutral molecule imidoylketene are produced.

rearrangement by comparison to other $C_3H_2NO^-$ isomers. Furthermore, the CID channel from I to IV (Figure 4) reveals a concurrent dissociation of both the N_1-C_2 and N_3-C_4 bonds, the most likely cleaved bonds in the uracil cation according to recent computational data.⁶³ This retro Diels Alder reaction results in the production of HNCO and deprotonated imidoylketene (III). From III, only 14.0 additional kcal mol⁻¹ are required to produce IV by decarboxylation. The reactivity of the anion, discussed in the following section, solidifies our identification of structure IV. However, the acidity and fragmentation processes discussed here clearly indicate that deprotonated imidoylketene (IV) is the dominant structure of $C_3H_2NO^-$.

4.3 Reactivity

Of the three major fragments derived from I, IV is the most reactive. We therefore focus our study on the reactivity of this ion, but include the qualitative trends that we observe for II and III here as well. Reactivity is characterized with several detected and potential interstellar species. Although no measurable reactions ($k_{\text{exp}} \leq 1 \times 10^{-13} \text{ cm}^3 \text{ s}^{-1}$) occurred between II, III, or IV with many of these molecules (NO, N₂O, CO, NH₃, O₂, and C₂H₄), reactions were observed for several sulfur-containing triatomic molecules (SO₂, OCS, and CS₂). II forms an adduct, and III participates in a solvent switching mechanism whereby each reagent replaces CO₂ on the ion. These general trends agree with our identification of the ion structures. II is expected to be a stable ring anion deprotonated on the nitrogen, agreeing with the trace ($<10^3$ ion counts s⁻¹) association products observed with carbon-centered reagents (OCS and CS₂) and the efficient association with the sulfur-centered species (SO₂). III is predicted to be a deprotonated carboxylic acid, supporting our observation of low intensity ($<10^3$ ion counts s⁻¹) solvent-switching products corresponding to the replacement of CO₂ with SO₂, OCS, and CS₂ on the reagent ion. The reactions examined with IV are measured quantitatively and discussed in detail below.

The observed ionic products, reaction rate constants (k_{exp}) and reaction efficiencies ($k_{\text{exp}}/k_{\text{col}}$) for IV with SO₂, OCS, and CS₂ are summarized in Table 2. Reaction efficiencies are expressed as the ratio of the reaction rate constant and the collision rate constant, determined by parametrized trajectory theory⁶⁴ for polar and Langevin⁶⁵ for nonpolar neutral reagents. The error reported in this table represents the precision of each measurement, defined as one standard deviation of the experimental mean. Additional systematic errors of our modified instrumental setup are approximately $\pm 30\%$. Also, theoretical calculations (B3LYP/6-311++G(d,p)) illustrate the largest TS barriers (TS in Table 2) and overall enthalpy changes for

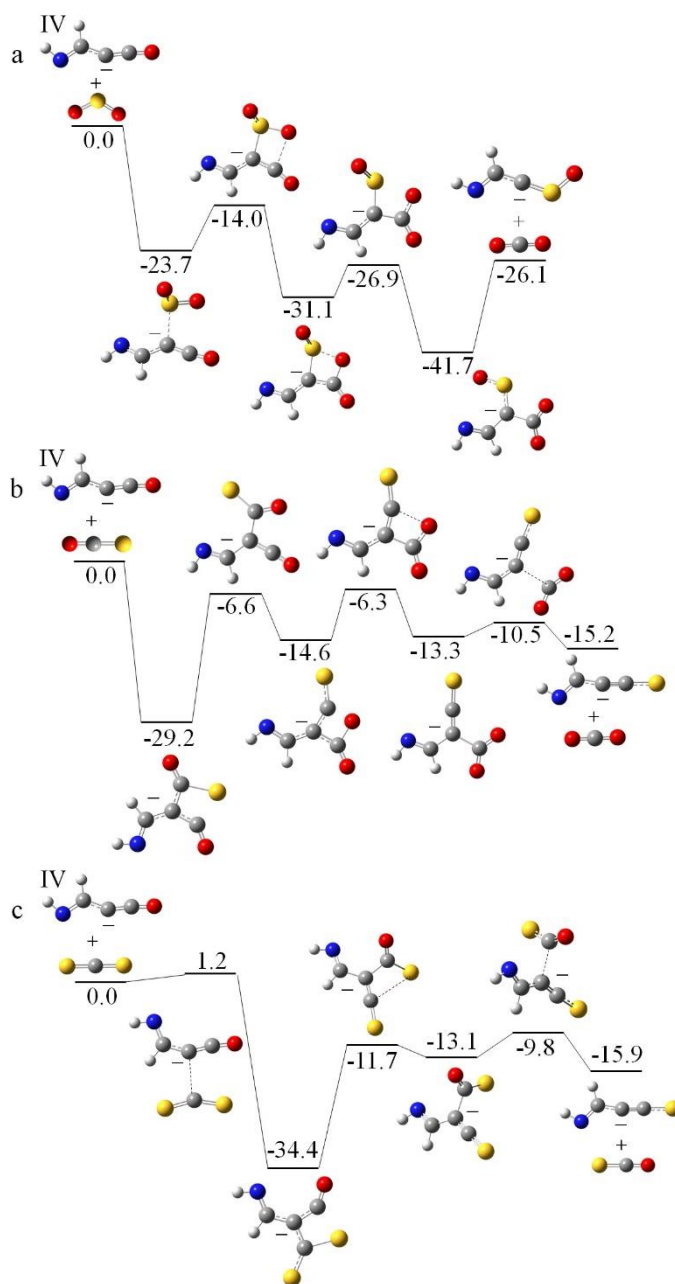


Figure 6. Deprotonated imidoylketene (IV) reacts similarly with SO₂ (a) and OCS (b) to produce CO₂. Deprotonated imidoylketene (IV) and CS₂ (c) do not react with a measurable rate constant to produce OCS and C₃H₂NS⁻ due to a small barrier (+1.2 kcal mol⁻¹). Units are in kcal mol⁻¹ and all species are calculated at the B3LYP/6-311++G(d,p) level of theory (ΔH_{0K}).

Table 2. Deprotonated Imidoylketene (IV) Reactivity

Neutral Reagent	Products	k_{exp} ($10^{-11} \text{ cm}^3 \text{ s}^{-1}$)	$k_{\text{exp}}/k_{\text{col}}$	TS ¹	ΔH_{0K} ¹
SO ₂	C ₂ H ₂ NOS ⁻ + CO ₂ ²	89 ± 14	0.56	-14.0	-26.2
OCS	C ₃ H ₂ NS ⁻ + CO ₂ ³	0.59 ± 0.06	0.0050	-6.3	-15.2
CS ₂	C ₃ H ₂ NS ⁻ + OCS ⁴	≤ 0.01	-	+1.2	-15.9

¹ All calculations are performed at the B3LYP/6-311++G(d,p) level of theory and results are reported in kcal mol⁻¹.

² A secondary product (C₂H₂NOS⁻–SO₂ adduct ion) is also observed. Only primary products are included in our analysis.

³ Adduct ions (C₃H₂NO⁻–OCS) are observed in trace amounts ($<10^3$ ion counts s⁻¹).

⁴ C₃H₂NS⁻ is observed in trace amounts ($<10^3$ ion counts s⁻¹).

each reaction pathway at 0 K. Even though ionic products are observed in all three cases, only the reactions with SO₂ and OCS were experimentally measurable, resulting in an upper limit for the reaction rate constant with CS₂.

From Table 2, a number of interesting observations can be made regarding the overall kinetics and thermodynamics of these reactions. As the largest TS barrier increases in energy from -14.0 to -6.3 kcal mol⁻¹, the overall reaction efficiency expectedly decreases dramatically, from 0.56 to 0.0050. Barriers even slightly above the energy of the reactants (+1.2 kcal mol⁻¹) leave only trace observable ion products and no measurable reaction rate constant. This verifies that ions in the modified ion trap apparatus are near-thermal.⁴⁸ Finally, the sulfur-centered reagent (SO₂) displays a significantly higher reaction efficiency than either of the carbon-centered reagents (OCS and CS₂), likely due to the bent geometry and increased molecular polarity of SO₂.

A more in depth look at these reactions is provided by potential energy diagrams. A direct comparison between the SO₂ (a) and OCS (b) reactions is shown in Figure 6. These reactions are similar in that they both involve the formation of an adduct ion and the subsequent transfer of an O atom from the neutral reagent molecule to the terminal CO on IV. This results in the eventual production of CO₂ from the adduct ion complex. Important differences in these diagrams are the increased barrier heights and the decreased overall exothermicity of the reaction with OCS, leading to a reaction efficiency two orders of magnitude below that of SO₂ (Table 2). Adding to this inefficiency, the OCS molecule forms a stable reactant complex rotated 180° with respect to its reactive geometry to produce CO₂. The first barrier shown in Figure 6b (-6.6 kcal mol⁻¹) in fact represents two TS structures and an optimized geometry all within 0.1 kcal mol⁻¹ of one another. This flat section of the potential energy surface certainly contributes to the overall inefficiency of this reaction. Notably, the more common reaction observed with OCS reagents, sulfur atom transfer,⁶⁶ is not observed here. Our calculations show that this process is in fact 8.1 kcal mol⁻¹ endothermic (ΔH_{0K}) and therefore not feasible within our ion trap apparatus.

The reaction rate constant is immeasurably slow ($k_{exp} \leq 1 \times 10^{-13} \text{ cm}^3 \text{ s}^{-1}$) between IV and CS₂, although trace (<10³ ion counts s⁻¹) product ions are visible in the mass spectrum. The initial barrier (+1.2 kcal mol⁻¹) resulting from the approach of CS₂ to the negatively charged C atom of IV is high enough to slow down the reaction significantly. The calculated potential energy diagram for this reaction is presented in Figure 6c. Following the initial barrier, a mechanism analogous to the other sulfur-containing reagents (Figure 6a and 6b) is shown, producing OCS rather than CO₂ through a sulfur atom transfer to the terminal CO of the ion.

4.4 Astrochemical Relevance

Fragmentation can be considered the reverse of synthesis. Therefore, the products of a fragmentation process lend insights into possible precursors. In considering Figure 2, most of the neutral fragments that are formed have been detected in the ISM: CO₂, HNCO, and HNC.⁶⁷⁻⁶⁹ HNCO (isocyanic acid) has been detected in many areas of the ISM and for this reason is used as an environmental diagnostic for different interstellar regions.^{70, 71} The ionic CID

products observed in this study involve one detected (OCN⁻)^{43, 72} and several potential (II, III, IV, and HC₂O⁻) interstellar species. The OCN⁻ anion is present in interstellar ices,⁴³ supporting the prospect of uracil formation in ice mantles. Figure 5 specifically addresses the fragmentation of deprotonated uracil, which forms OCN⁻ and imidoylketene. This highlights the importance of further interstellar searches for uracil and imidoylketene, particularly in dense clouds where N-heterocycles and larger organics are predicted to be stable.⁷³

Deprotonated imidoylketene reactivity is also astrochemically relevant. This molecule can isomerize into many different heterocyclic structures including azoles,^{74, 75} and has been long recognized as a molecule of cosmochemical interest.⁴⁴ The ability of imidoylketene to form ring structures suggests its involvement in N-heterocycle synthesis.⁴¹ Additionally, the future interstellar detection of imidoylketene is promising due to the detection of its isomer, oxiranecarbonitrile.^{46, 47} Our study unveils interesting reactions for deprotonated imidoylketene (IV) with interstellar triatomic sulfur-containing molecules (OCS and SO₂)^{76, 77} involving association and subsequent CO₂ loss. These reactions provide important suggestions for gas-phase sulfur incorporation into larger organic species.

5. Conclusions

According to NASA, the origin of terrestrial life is among the three basic topics addressed by the field of astrobiology.⁷⁸ The study of nucleobases, from their reactivity and fragmentation to their prebiotic synthesis routes, is essential in this effort. For the Murchison, Murray, and Orgueil carbonaceous meteorites, uracil was the only pyrimidine nucleobase detected in all three,¹¹ supporting the theory of its exogenous synthesis and delivery to early earth.³ Interstellar detections of nucleobases remain inconclusive, although the abundance of interstellar nitrogen and aromatic organics is well known.²² These data have motivated the proposal of many prebiotic formation pathways to uracil,^{6-11, 13, 14} but anions are commonly missing reagents in these endeavors.

Recent studies have used fragmentation to reveal possible biomolecule synthesis routes.^{30, 31} Our investigation similarly stems from the dissociation of deprotonated uracil-5-carboxylic acid (C₅H₃N₂O₄⁻) to decipher important uracil precursors. Through decarboxylation and HNCO loss from C₅H₃N₂O₄⁻, N₁ deprotonated uracil (C₄H₃N₂O₂⁻), deprotonated imidoylketene carboxylic acid (C₄H₂NO₃⁻), and deprotonated imidoylketene (C₃H₂NO⁻) are produced in a modified Finnigan LCQ Deca XP Plus ion trap. The structures of these ions are verified through theoretical calculations, experimental acidity bracketing, and further fragmentation. Our experimental acidity brackets of C₅H₃N₂O₄⁻, C₄H₃N₂O₂⁻, and C₃H₂NO⁻ (ΔH°_{acid} , < 323.540 ± 0.050, 336.9 ± 2.1 kcal mol⁻¹, and 357.5 ± 6.1 kcal mol⁻¹ respectively, agree well with calculated values for our predicted structures of these ions. Further fragmentation results also support our structural identifications. N₁ deprotonated uracil fragments to form OCN⁻ and imidoylketene, two possible uracil precursors. Ice mantles may provide favorable conditions for complex organic molecule formation,⁵ and the presence of OCN⁻ in interstellar ices provides an essential ingredient for uracil synthesis there. Deprotonated imidoylketene carboxylic acid loses CO₂ to form

deprotonated imidoyleketene, which subsequently dissociates into HNC and HC_2O^- . Previous studies have reported comparable fragments for positive ion studies of uracil,³⁷ and computational explorations of uracil bond strengths predict that our fragments are reasonable.⁶³ Notably, imidoyleketene itself is a molecule of cosmochemical interest⁴⁴ that has been proposed to react to form larger cyclic species, supporting its potential as an N-heterocycle precursor.⁴⁵

The reactivity of the three primary fragments ($\text{C}_3\text{H}_2\text{NO}^-$, $\text{C}_4\text{H}_3\text{N}_2\text{O}_2^-$, and $\text{C}_4\text{H}_2\text{NO}_3^-$) are examined with a set of neutral reagents including several detected interstellar molecules (SO_2 , OCS, CS_2 , NO, N_2O , CO, NH_3 , O_2 , and C_2H_4). An interesting pattern of reactivity is observed for the sulfur-containing triatomic reagents. N_1 deprotonated uracil efficiently forms adduct ions with SO_2 , as opposed to carbon-centered reagents which displayed only trace products. Deprotonated imidoyleketene carboxylic acid displays trace levels of solvent-switching products with all three triatomic species, supporting our structural identification of the anion. Finally, a more quantitative examination of deprotonated imidoyleketene reveals a mechanism involving association and CO_2 production. SO_2 reacts very efficiently ($k_{\text{exp}}/k_{\text{col}} = 0.56$), and the largest calculated barrier to its reaction is $14.0 \text{ kcal mol}^{-1}$ below the energy of the reactants. The potential energy surface for the analogous OCS reaction is much flatter and involves higher overall barriers ($\geq 6.3 \text{ kcal mol}^{-1}$ below the reactant energy), leading to a lower overall reaction efficiency (0.0050). Product ions were visible in trace amounts for the reaction with CS_2 , but the reaction rate constant was immeasurably small ($k_{\text{exp}} \leq 1 \times 10^{-13} \text{ cm}^3 \text{ s}^{-1}$). The calculated barrier of $+1.2 \text{ kcal mol}^{-1}$ along the potential energy surface of this reaction is sufficient to prevent the reaction of the near-thermal ions in our ion trap apparatus.

In summary, we have outlined a comprehensive examination of the anionic derivatives of uracil. Our data support the involvement of anions in more complex biomolecule formation, though they are often overlooked as reagents in prebiotic syntheses. The fragmentation and reaction processes reported here yield many interstellar ions and neutral molecules, providing important connections between these species. Along with the continued search for nucleobases and other N-heterocycles, these data motivate the further inclusion of anions in proposed prebiotic formation routes to nucleobases.

Acknowledgements

We thank Dr. Jennifer Herbst, Mr. Nicholas Demarais, and Mr. Charles Nichols for their insights and contributions. We are grateful to the National Center for Supercomputing Applications for our access to TeraGrid Resources. This material is based upon work supported by a National Science Foundation (NSF) Graduate Research Fellowship under Grant No. DGE-1144083 and NSF Grant CHE-1300886. Any opinion, findings, and conclusions or recommendations expressed in this material are those of the authors and do not necessarily reflect the views of the National Science Foundation.

Notes and references

^a Department of Chemistry and Biochemistry, 215 UCB, University of Colorado, Boulder, CO 80309, USA.

^b Department of Astrophysical and Planetary Sciences, 391 UCB, University of Colorado, Boulder, CO 80309, USA.

^c Center for Astrophysics and Space Astronomy, 389 UCB, University of Colorado, Boulder, CO 80309, USA.

Electronic Supplementary Information (ESI) available: [Figures S1-S3 pdf document included]. See DOI: 10.1039/b000000x/

References

1. L. E. Orgel, *Critical Reviews in Biochemistry and Molecular Biology*, 2004, **39**, 99-123.
2. K. Kobayashi, Y. Takano, H. Masuda, H. Tonishi, T. Kaneko, H. Hashimoto and T. Saito, in *Space Life Sciences: Search for Signatures of Life, and Space Flight Environmental Effects on the Nervous System*, eds. G. Horneck, A. C. Levasseur-Regourd, B. M. Rabin and K. B. Slenzka, 2004, vol. 33, pp. 1277-1281.
3. C. Chyba and C. Sagan, *Nature*, 1992, **355**, 125-132.
4. J. Oro, *Nature*, 1961, **190**, 389-390.
5. E. Herbst, *Physical Chemistry Chemical Physics*, 2014, **16**, 3344-3359.
6. A. Ricca, C. W. Bauschlicher and E. L. O. Bakes, *Icarus*, 2001, **154**, 516-521.
7. V. P. Gupta, P. Tandon and P. Mishra, *Advances in Space Research*, 2013, **51**, 797-811.
8. A. Horn, H. Mollendal and J.-C. Guillemin, *Journal of Physical Chemistry A*, 2008, **112**, 11009-11016.
9. P. P. Bera, T. J. Lee and H. F. Schaefer, III, *Journal of Chemical Physics*, 2009, **131**, 074303.
10. P. P. Bera, M. Nuevo, S. N. Milam, S. A. Sandford and T. J. Lee, *Journal of Chemical Physics*, 2010, **133**, 104303.
11. M. Nuevo, S. N. Milam, S. A. Sandford, J. E. Elsila and J. P. Dworkin, *Astrobiology*, 2009, **9**, 683-695.
12. A. J. Remijan, L. E. Snyder, B. A. McGuire, H.-L. Kuo, L. W. Looney, D. N. Friedel, G. Y. Golubiatnikov, F. J. Lovas, V. V. Ilyushin, E. A. Alekseev, S. F. Dyubko, B. J. McCall and J. M. Hollis, *Astrophysical Journal*, 2014, **783**, 77.
13. T. Wang and J. H. Bowie, *Organic & Biomolecular Chemistry*, 2012, **10**, 652-662.
14. M. P. Robertson and S. L. Miller, *Nature*, 1995, **375**, 772-774.
15. H. Gupta, C. A. Gottlieb, V. Lattanzi, J. C. Pearson and M. C. McCarthy, *Astrophysical Journal Letters*, 2013, **778**, L1.
16. G. Danger, F. Duvernay, P. Theule, F. Borget, J. C. Guillemin and T. Chiavassa, *Astronomy & Astrophysics*, 2013, **549**, A93.
17. C. Barckholtz, T. P. Snow and V. M. Bierbaum, *Astrophysical Journal*, 2001, **547**, L171-L174.
18. B. Eichelberger, T. P. Snow, C. Barckholtz and V. M. Bierbaum, *Astrophysical Journal*, 2007, **667**, 1283-1289.
19. R. Hayatsu, *Science*, 1964, **146**, 1291-1293.
20. C. E. Folsome, J. Lawless, M. Romiez and C. Ponnampe, *Nature*, 1971, **232**, 108-109.
21. P. G. Stoks and A. W. Schwartz, *Nature*, 1979, **282**, 709-710.

22. Z. Peeters, O. Botta, S. B. Charnley, R. Ruitkamp and P. Ehrenfreund, *Astrophysical Journal*, 2003, **593**, L129-L132.
23. S. Brunken, M. C. McCarthy, P. Thaddeus, P. D. Godfrey and R. D. Brown, *Astronomy & Astrophysics*, 2006, **459**, 317-320.
24. E. Herbst and E. F. van Dishoeck, in *Annual Review of Astronomy and Astrophysics*, Vol 47, eds. R. Blandford, J. Kormendy and E. VanDishoeck, 2009, vol. 47, pp. 427-480.
25. Y. J. Kuan, S. B. Charnley, H. C. Huang, W. L. Tseng and Z. Kisiel, *Astrophysical Journal*, 2003, **593**, 848-867.
26. Y. J. Kuan, S. B. Charnley, H. C. Huang, Z. Kisiel, P. Ehrenfreund, W. L. Tseng and C. H. Yan, *Space Life Sciences: Steps toward Origin(s) of Life*, 2004, **33**, 31-39.
27. Y. J. Kuan, H. C. Huang, S. B. Charnley, W. L. Tseng, L. E. Snyder, P. Ehrenfreund, Z. Kisiel, S. Thorwirth, R. K. Bohn and T. L. Wilson, *Bioastronomy 2002: Life among the Stars*, 2004, 185-188.
28. S. B. Charnley, Y. J. Kuan, H. C. Huang, O. Botta, H. M. Butner, N. Cox, D. Despois, P. Ehrenfreund, Z. Kisiel, Y. Y. Lee, A. J. Markwick, Z. Peeters and S. D. Rodgers, *Space Life Sciences: Astrobiology: Steps toward Origin of Life and Titan before Cassini*, 2005, **36**, 137-145.
29. Y. J. Kuan, C. H. Yan, S. B. Charnley, Z. Kisiel, P. Ehrenfreund and H. C. Huang, *Monthly Notices of the Royal Astronomical Society*, 2003, **345**, 650-656.
30. A. Simakov, G. B. S. Miller, A. J. C. Bunkan, M. R. Hoffmann and E. Uggerud, *Physical Chemistry Chemical Physics*, 2013, **15**, 16615-16625.
31. E. L. Zins, C. Pirim, L. Vettier, M. Chaboud and L. Krim, *International Journal of Mass Spectrometry*, 2013, **348**, 47-52.
32. Z. Lin, D. Talbi, E. Roueff, E. Herbst, N. Wehres, C. A. Cole, Z. Yang, T. P. Snow and V. M. Bierbaum, *Astrophysical Journal*, 2013, **765**, 80.
33. C. A. Cole, N. Wehres, Z. Yang, D. L. Thomsen, T. P. Snow and V. M. Bierbaum, *Astrophysical Journal Letters*, 2012, **754**, L5.
34. Z. Yang, C. A. Cole, O. Martinez, Jr., M. Y. Carpenter, T. P. Snow and V. M. Bierbaum, *Astrophysical Journal*, 2011, **739**, 19.
35. C. A. Cole, N. J. Demarais, Z. Yang, T. P. Snow and V. M. Bierbaum, *Astrophysical Journal*, 2013, **779**, 181.
36. C. C. Nelson and J. A. McCloskey, *Journal of the American Society for Mass Spectrometry*, 1994, **5**, 339-349.
37. D. G. Beach and W. Gabryelski, *Journal of the American Society for Mass Spectrometry*, 2012, **23**, 858-868.
38. R. Rodriguez-Fernandez, S. A. Vazquez and E. Martinez-Nunez, *Physical Chemistry Chemical Physics*, 2013, **15**, 7628-7637.
39. B. Barc, M. Ryszka, J. Spurrell, M. Dampc, P. Limao-Vieira, R. Parajuli, N. J. Mason and S. Eden, *Journal of Chemical Physics*, 2013, **139**, 244311.
40. F. F. da Silva, C. Matias, D. Almeida, G. Garcia, O. Ingolfsson, H. D. Flosadottir, B. Omarsson, S. Ptasinska, B. Puschnigg, P. Scheier, P. Limao-Vieira and S. Denifl, *Journal of the American Society for Mass Spectrometry*, 2013, **24**, 1787-1797.
41. J. Tabet, S. Eden, S. Feil, H. Abdoul-Carime, B. Farizon, M. Farizon, S. Ouaskit and T. D. Mark, *Physical Review A*, 2010, **81**, 012711.
42. J. de Vries, R. Hoekstra, R. Morgenstern and T. Schlathoelter, *Physica Scripta*, 2004, **T110**, 336-339.
43. B. T. Soifer, R. C. Puetter, R. W. Russell, S. P. Willner, P. M. Harvey and F. C. Gillett, *Astrophysical Journal*, 1979, **232**, L53-L57.
44. C. Wentrup, H. Briehl, P. Lorencak, U. J. Vogelbacher, H. W. Winter, A. Maquestiau and R. Flammang, *Journal of the American Chemical Society*, 1988, **110**, 1337-1343.
45. A. Pena-Gallego, J. Rodriguez-Otero and E. M. Cabaleiro-Lago, *Tetrahedron*, 2007, **63**, 4937-4943.
46. J. E. Dickens, W. M. Irvine, M. Ohishi, G. Arrhenius, S. Pitsch, A. Bauder, F. Muller and A. Eschenmoser, *Origins of Life and Evolution of Biospheres*, 1996, **26**, 97-110.
47. M. Behnke, I. Medvedev, M. Winnewisser, F. C. De Lucia and E. Herbst, *Astrophysical Journal Supplement Series*, 2004, **152**, 97-101.
48. S. Gronert, *Journal of the American Society for Mass Spectrometry*, 1998, **9**, 845-848.
49. S. K. Koehn, N. L. Tran, S. Gronert and W. M. Wu, *Journal of the American Chemical Society*, 2010, **132**, 390-395.
50. N. A. Senger, C. E. Bliss, J. R. Keeffe, S. Gronert and W. Wu, *Tetrahedron*, 2013, **69**, 5287-5292.
51. S. Gronert, *Mass Spectrometry Reviews*, 2005, **24**, 100-120.
52. G. E. Reid, R. A. J. O'Hair, M. L. Styles, W. D. McFadyen and R. J. Simpson, *Rapid Communications in Mass Spectrometry*, 1998, **12**, 1701-1708.
53. S. Gronert, C. H. DePuy and V. M. Bierbaum, *Journal of the American Chemical Society*, 1991, **113**, 4009-4010.
54. C. H. DePuy, S. Gronert, A. Mullin and V. M. Bierbaum, *Journal of the American Chemical Society*, 1990, **112**, 8650-8655.
55. M. J. Frisch, G. W. Trucks, H. B. Schlegel, G. E. Scuseria, M. A. Robb, J. R. Cheeseman, J. A. Montgomery, T. Vreven, K. N. Kudin, J. C. Burant, J. M. Millam, S. S. Iyengar, J. Tomasi, V. Barone, B. Mennucci, M. Cossi, G. Scalmani, N. Rega, G. A. Petersson, H. Nakatsuji, M. Hada, M. Ehara, K. Toyota, R. Fukuda, J. Hasegawa, M. Ishida, T. Nakajima, Y. Honda, O. Kitao, H. Nakai, M. Klene, X. Li, J. E. Knox, H. P. Hratchian, J. B. Cross, V. Bakken, C. Adamo, J. Jaramillo, R. Gomperts, R. E. Stratmann, O. Yazyev, A. J. Austin, R. Cammi, C. Pomelli, J. W. Ochterski, P. Y. Ayala, K. Morokuma, G. A. Voth, P. Salvador, J. J. Dannenberg, V. G. Zakrzewski, S. Dapprich, A. D. Daniels, M. C. Strain, O. Farkas, D. K. Malick, A. D. Rabuck, K. Raghavachari, J. B. Foresman, J. V. Ortiz, Q. Cui, A. G. Baboul, S. Clifford, J. Cioslowski, B. B. Stefanov, G. Liu, A. Liashenko, P. Piskorz, I. Komaromi, R. L. Martin, D. J. Fox, T. Keith, A. Laham, C. Y. Peng, A. Nanayakkara, M. Challacombe, P. M. W. Gill, B. Johnson, W. Chen, M. W. Wong, C. Gonzalez and J. A. Pople, 2003.
56. M. J. Frisch, G. W. Trucks, H. B. Schlegel, G. E. Scuseria, M. A. Robb, J. R. Cheeseman, G. Scalmani, V. Barone, B. Mennucci, G. A. Petersson, H. Nakatsuji, M. Caricato, X. Li, H. P. Hratchian, A. F. Izmaylov, J. Bloino, G. Zheng, J. L. Sonnenberg, M. Hada, M. Ehara, K. Toyota, R. Fukuda, J. Hasegawa, M. Ishida, T. Nakajima, Y. Honda, O. Kitao, H. Nakai, T. Vreven, Jr, J. E. Peralta, F. Ogliaro, M. Bearpark, J. J. Heyd, E. Brothers, K. N. Kudin, V. N. Staroverov, R. Kobayashi, J. Normand, K. Raghavachari, A. Rendell, J. C. Burant, S. S. Iyengar, J. Tomasi, M. Cossi, N. Rega, J. M. Millam, M. Klene, J. E. Knox, J. B. Cross, V. Bakken, C. Adamo, J. Jaramillo, R. Gomperts, R. E.

- Stratmann, O. Yazyev, A. J. Austin, R. Cammi, C. Pomelli, J. W. Ochterski, R. L. Martin, K. Morokuma, V. G. Zakrzewski, G. A. Voth, P. Salvador, J. J. Dannenberg, S. Dapprich, A. D. Daniels, Farkas, J. B. Foresman, J. V. Ortiz, J. Cioslowski and D. J. Fox, *Gaussian 09 Revision A.02*, Gaussian Inc. Wallingford CT 2009, 2009.
57. S. S. Bokatzian-Johnson, M. L. Stover, D. A. Dixon and C. J. Cassady, *Journal of Physical Chemistry B*, 2012, **116**, 14844-14858.
58. S. Kumari, C. L. Devi, S. Prabhakar, K. Bhanuprakash and M. Vairaman, *Journal of the American Society for Mass Spectrometry*, 2010, **21**, 136-143.
59. *NIST Chemistry WebBook, NIST Standard Reference Database Number 69*, National Institute of Standards and Technology, <http://webbook.nist.gov/chemistry/>, accessed 12 Dec 2013.
60. Y. Q. Huang and H. I. Kenttämä, *Journal of Physical Chemistry A*, 2003, **107**, 4893-4897.
61. C. H. DePuy, V. M. Bierbaum, R. Damrauer and J. A. Soderquist, *Journal of the American Chemical Society*, 1985, **107**, 3385-3386.
62. A. J. Cohen, P. Mori-Sanchez and W. Yang, *Science*, 2008, **321**, 792-794.
63. L. S. Arani, P. Mignon, H. Abdoul-Carime, B. Farizon, M. Farizon and H. Chermette, *Physical Chemistry Chemical Physics*, 2012, **14**, 9855-9870.
64. T. Su and W. J. Chesnavich, *Journal of Chemical Physics*, 1982, **76**, 5183-5185.
65. G. Gioumousis and D. P. Stevenson, *Journal of Chemical Physics*, 1958, **29**, 294-299.
66. C. H. DePuy and V. M. Bierbaum, *Tetrahedron Letters*, 1981, **22**, 5129-5130.
67. L. B. d'Hendecourt and M. J. Demuizon, *Astronomy & Astrophysics*, 1989, **223**, L5-L8.
68. L. E. Snyder and D. Buhl, *Annals of the New York Academy of Sciences*, 1972, **194**, 17-24.
69. J. H. Lacy, N. J. Evans, J. M. Achtermann, D. E. Bruce, J. F. Arens and J. S. Carr, *Astrophysical Journal*, 1989, **342**, L43-L46.
70. D. Quan, E. Herbst, Y. Osamura and E. Roueff, *Astrophysical Journal*, 2010, **725**, 2101-2109.
71. D. M. Tideswell, G. A. Fuller, T. J. Millar and A. J. Markwick, *Astronomy & Astrophysics*, 2010, **510**, A85.
72. V. Lattanzi, C. A. Gottlieb, P. Thaddeus, S. Thorwirth and M. C. McCarthy, *Astrophysical Journal*, 2010, **720**, 1717-1720.
73. Z. Peeters, O. Botta, S. B. Charnley, Z. Kisiel, Y. J. Kuan and P. Ehrenfreund, *Astronomy & Astrophysics*, 2005, **433**, 583-590.
74. M. T. Nguyen, T. K. Ha and R. A. M. Oferrall, *Journal of Organic Chemistry*, 1990, **55**, 3251-3256.
75. S. Vijayakumar and P. Kolandaivel, *Molecular Physics*, 2006, **104**, 1401-1411.
76. K. B. Jefferts, A. A. Penzias, R. W. Wilson and P. M. Solomon, *Astrophysical Journal*, 1971, **168**, L111-L113.
77. L. E. Snyder, J. M. Hollis, B. L. Ulich, F. J. Lovas, D. R. Johnson and D. Buhl, *Astrophysical Journal*, 1975, **198**, L81-L84.
78. D. J. D. Marais, J. A. Nuth, III, L. J. Allamandola, A. P. Boss, J. D. Farmer, T. M. Hoehler, B. M. Jakosky, V. S. Meadows, A. Pohorille, B. Runnegar and A. M. Spormann, *Astrobiology*, 2008, **8**, 715-730.